Hindawi
Journal of Nanomaterials
Volume 2020, Article ID 4090856, 12 pages
https://doi.org/10.1155/2020/4090856

Research Article

Evaluation of an Epoxy-Based Nanosilicacomposite Lining in H_2SO_4 Solution for Anticorrosion of Sewerage Concrete Structures

Chau Van Dinh

Faculty of Engineering Physics and Nanotechnology, University of Engineering and Technology, Vietnam National University in Hanoi, No. 144 Xuan Thuy Street, Hanoi, Vietnam

Correspondence should be addressed to Chau Van Dinh; dinhchau@vnu.edu.vn

Received 12 February 2020; Accepted 15 April 2020; Published 4 May 2020

Academic Editor: David Cornu

This work presents the performance of a SiO_2-epoxy nanocomposite lining for the anticorrosion of the concrete structures in sewer networks. Nanocomposite lining on the concrete substrate surface of the 15 phr (part per hundred epoxy resin) amine-cured epoxy polymer containing 3.0 phr of nano-SiO_2 was prepared by intercalating epoxy into the SiO_2 via direct mixing process. The silica exfoliation was monitored by X-ray diffraction (XRD) and transmission electron microscopy (TEM). The barrier feature of epoxy the base nanocomposite against water and sulfuric acid solution was evaluated. The results showed that the nanocomposite lining was of a great barrier against these corrosive environments due to the intercalation and exfoliation caused by the dispersion of the SiO_2 nanoparticles into the epoxy matrix. The rate of the H_2SO_4 into the nanocomposite lining was also investigated by measurement of the depth of the sulfur element penetrated layer using the coupled Scanning Electron Microscopy (SEM)/Energy dispersive X-ray spectrometer (EDS). Deterioration behavior of the adhesion strength of the nanocomposite lining was studied. The nanocomposite lining shows a significant improvement of bond strength in comparison to the neat epoxy lining. The durability of the nanocomposite lining adhesion when the lining systems exposed to water and the sulfuric acid solution is also improved significantly.

1. Introduction

Nowadays, as a part of living standards, sewer systems are implemented for the collection and transportation of wastewater to treatment facilities. Most of these piping systems are constructed of concrete since concrete is compatible with the environment and the cost-effectiveness. For example, in Australia, it is approximately 40% of 117,000 km of sewerage pipeline constructed from concrete while in Germany, concrete material accounted for 46% of the material structure used for sewer networks [1, 2]. However, sewer concrete structures are rapidly degraded because of the acidic environments generated by bacterial activities [3]. This degradation is well-known as microbially induced concrete corrosion [4–6]. In sewer networks, hydrogen sulfide formed by sulfate-reducing bacteria (SRB) is released to the sewer air, absorbed/adsorbed into the moisture layer on the concrete walls exposed to air, then, it was oxidized to sulfuric acid by the activity of sulfide-oxidizing bacteria (SOB), corroded concrete [1]. The sulfuric acid reacts with the silicate and carbonate compounds to form gypsum via the following reactions:

$$\begin{aligned} H_2SO_4 + CaO.SiO_2.2H_2O &\longrightarrow CaSO_4 + Si(OH)_4 + H_2O \\ H_2SO_4 + CaCO_3 &\longrightarrow CaSO_4 + H_2CO_3 \\ H_2SO_4 + Ca(OH)_2 &\longrightarrow CaSO_4 + H_2O \end{aligned} \quad (1)$$

The formation of gypsum leads to an increase of approximately 124% in volume weakened the concrete structure [7]. More destructively, the subsequent reaction between gypsum and tricalcium aluminates within the cement matrix took place and forms the mineral Ettringite. Since the mineral Ettringite creates an extremely high expansion in volume,

up to 700% [7, 8], the internal cracking and pitting of the concrete occurs, making an increase of the surface reaction area and then facilitates easier penetration of moisture, acids, and microorganisms into the concrete structure. The corrosion rate of sewer concrete structures is in a range of 1 to 10 mm/year up to 10 mm/year [9]. Loss in concrete volume, cracking, and even collapse of sewer concrete structure are reported by this corrosion process [6, 9–13]. Globally, billions of dollars per year are spent on premature replacement or rehabilitation of the corrosion sewer concrete structures [14].

Current strategies for controlling sewer corrosion are focused on (i) preventing H_2S production and its partition from the sewer liquid phase through the dosing of antimicrobials, iron salts, pH elevating compounds, and oxidants (i.e., oxygen and nitrate) to the sewage; (ii) reducing the H_2S concentration in sewer air through forced ventilation; (iii) and applying the surface treatment on concrete sewers [14]. Among these strategies, the surface lining/coating can be used to provide long-term effective protection of concrete structures especially against corrosion [3, 15, 16]. Polymeric coating/lining protective materials (e.g., polyurethane, epoxy, and chlorinated rubber) avoid concrete deterioration exposed to sulfuric acid [16]. Epoxy is a broad family of chemicals with differing physical and chemical properties. The main features that impact on its durability include curing agents (e.g., amine, amide, cycloaliphatic), solvents, and fillers. Epoxies generally have excellent mechanical properties and high chemical resistance [17]; hence, the resins have been widely applied in corrosion protection. Another advantage of these materials in the lining application is their easily being lined on the concrete structure without the requirement of the high-pressure equipment due to its low viscosity. However, fully cured epoxy resins formulations are brittle and have high water uptake [18]. To overcome those disadvantages, a dispersion of inorganic nanoparticles into an epoxy continuous phase may improve barrier property to the sulfuric acid solution and moisture. The reports for epoxy/TiO_2 and Latex/silica conducted by Rong et al. and Ng et al. show that the use of nanofillers has advantages, such as improvements in scratch, abrasion, heat, radiation, and swelling resistance; a decrease in water permeability; and, an increase in hardness, weatherability, and elastic modulus when compared to conventional organic coatings containing micro fillers [19–21]. Shi et al. in the study of the effect of nanoparticles on the anticorrosion and mechanical properties of epoxy coating concluded that the presence of silica nanoparticles was the most effective way of enhancing the mechanical strength of coatings and the second most effective in terms of the improvement of anticorrosive properties [22]. In another study, an improvement in the mechanical properties (wear and impact resistance) of nanosilica-based coatings as compared with their micro silica-based equivalents was reported [23]. Nikje et al. prepared SiO2-reinforced epoxy composite coatings using in situ polymerization and pointed out an increase in both the thermal and mechanical properties of the modified coating in comparison to unmodified coatings [24]. A basalt flake modified epoxy coatings incorporated with 3% nanosilica showed excellent chemical and mechanical performance in a report published by Luo et al. [25].

When an epoxy-silica nanocomposite lining exposure long to the environment for a long time, degradation processes such as chemical degradation, reduction of mechanical properties, etc. may occur. The environment penetration into a polymer composite is influenced by the composite's characteristics such as density and the order of pore, defects or contamination, and the polymer-environment affinity [26, 27]. In the studies of liquid molecular transport into a polymer membrane, diffusion has been classified as Type I (Fickian type), Type II (relaxation-controlled type), and non-Fickian (anomalous type) [28–32]. Penetrant molecules diffuse into the membrane until the concentration is equal over the whole of the membrane (saturation state). When Fickian diffusion is assumed, the time-dependent relative concentration of the liquids into the polymer membrane can be expressed by Equation (2) [33].

$$\frac{C_{(t,x)}}{C_\infty} = 1 - \frac{4}{\pi}\sum_{m=0}^{\infty}\frac{1}{(2m+1)}\exp\left[-\frac{D(2m+1)^2\pi^2 t}{l^2}\right] * \sin\left[\frac{(2m+1)\pi x}{h}\right], \quad (2)$$

where $C(t,x)$ and C_∞ are the concentrations of the liquid inside the membrane at time t, position x, and saturate state; D is diffusivity, which depends on the nature of liquid-polymer interactions; and h is the thickness of the membrane. The boundary conditions for solving Equation (2) are: $C = 0$ when $t = 0$, $0 \le x \le h$; $C = C_\infty$ when $t > 0$, $x = 0$, $x = h$; and $\partial C/\partial x = 0$ when $x = 0$, $t > 0$. The diffusion coefficient has been calculated by Equation (3) [34].

$$\frac{M_t}{M_\infty} = \frac{4}{h}\sqrt{\frac{Dt}{\pi}}, \quad (3)$$

where M_t and M_∞ are the mass uptake at time t and saturation state, respectively. The diffusivity can be calculated from the initial slope of the environmental uptake M_t/M_∞ versus time ($t^{1/2}/h$) as

$$D = \frac{\pi}{16}\left(\frac{M_t/M_\infty}{\sqrt{t}/h}\right)^2. \quad (4)$$

The environmental uptake content may predict by using the equation as follows [35]:

$$\frac{M_t}{M_\infty} = 1 - \exp\left[-7.3\left(\frac{Dt}{h^2}\right)^{0.75}\right]. \quad (5)$$

The high-order absorption of water or exposed environment is a major disadvantage of the lined layer. Furthermore, the absorbed water is considered as a main factor that resulted in the degradation of the functional, structural, and mechanical properties of the composites [36–38]. Therefore, the understanding of the diffusion behavior of water in a

particular epoxy-silica nanocomposite system is needed for the application of the material lining/coating industry.

This study reports our findings on the degradation of epoxy-silica nanocomposite lined on concrete substrate exposure to sulfuric acid solution for the purpose of the anticorrosion of sewerage concrete.

2. Materials and Methods

2.1. Materials. Nanosilica fillers branded Aerosil R812 from Evonik having an average diameter of 7 nm, a specific area of 260 m^2/g and purity > 99.8%. The surface of this material was modified with hexamethyldisilazane. The epoxy matrix was a mixture of a diglycidyl ether of bisphenol F (DGEBF) epoxy resin (EPOKUDO YDF-175, Kukdo Chemical), having an equivalent mass of 160-180 (grams of resin containing one gram equivalent of epoxide) and a polyetheramine curing agent (Jeffamine D230, Hunsman Corporation). The solvent used for nanocomposite processing was reagent grade toluene (Aldrich) with purity > 99.5%. Table 1 shows the mixture proportions for the protective lining materials.

2.2. Preparation of Immersion Samples. Free-standing nanocomposite sheets having 1.0 mm thickness of the 15 phr (part per hundred epoxy resin) amine-cured epoxy polymer containing 3.0 phr of nano-SiO_2 were prepared. The SiO_2 nanofillers were first sonicated in a large amount of toluene for 30 minutes using an 80 kHz tip sonicator. After adding epoxy resin, the nanofillers suspension was ultrasonicated by a magnetic stirrer at speed of 2500 rpm for 1 hour. The amine curing agent was then added to the suspension. The mixture stirred and sonicated continuously for another hour. After the mixing step, both the nanosilica-free and epoxy/nanosilica mixture was degassed for 1 hour at room temperature then drawn down on polyethylene terephthalate mold to form sheets. The sheets were cured at ambient conditions (24°C and 75% relative humidity approximately) for 72 hrs followed by postcuring for 4 hrs at 110°C in an air circulating oven. The immersion test samples having dimensions of $60 \times 25 \times 1.0$ mm were prepared from the fabricated sheets then dried up at 50°C for 72 hrs to ensure that the remaining moisture/gas was removed before used for immersion test. Unfilled (neat) epoxy sheets were also prepared in the same manner.

2.3. Preparation of Lining Specimens. The concrete substrates were cast from mix design (Table 2) prepared in compliance with the Vietnamese Standard [39]. The substrate's side length and thickness are $150 \times 150 \times 50$ mm. The substrates were cured in moist air for 24 hrs and then cured in lime-saturated water for 28 days. After curing, the substrates were dried in an oven at 60°C for 7 days to achieve similar and stable initial water content [40]. The top surface of the substrate slabs was disk-grinded to a roughness level corresponding to the concrete surface profile (CSP), as described by the International Concrete Repair Institute (ICRI) [41]. The degassed mixtures (prepared in the same manner as the sheet forming) drawn down on the sandblasted surfaces to form the lining film. The lining specimens then were cured at ambient conditions (24°C and 75% relative humidity approximately) for 72 hrs followed by postcuring for 4 hrs at 110°C in an air circulating oven. The thickness of the lining film was about 1.0 mm.

Table 1: Mixture proportions for the protective lining materials.

Sample	Mixture proportions (part per hundred resin—phr)		
	DGEBF	Curing agent	Nanosilica
NS-0	100	15	0
NS-3	100	15	3

2.4. Environmental Uptake Experiment. The mass uptake experiment was conducted using an apparatus as illustrated in Figure 1. The mass uptake of samples having dimension $60 \times 25 \times 1.0$ mm immersed separately in deionized water and 10 wt.% sulfuric acid medium at 30 and 50°C using constant temperature bath was measured by recording the amount of the solution absorbed within a fixed interval of immersion time. The samples were periodically taken out, wiped with filter paper to remove excess solution then were kept for 1 h at room temperature before their weights, the wet condition, were carried out. Solution content was determined by Equation (6).

$$M_t[\%] = \frac{W_t - W_0}{W_0}.100, \tag{6}$$

where M_t, W_t, and W_0 are the solution content at a time t, weight of the immersed sample at the time t, and initial weight, respectively.

2.5. Adhesion Degradation Test (Pull-Off Method). The epoxy-silica nanocomposite lined concrete substrates conducted to the degraded adhesion test as shown in Figure 2. The temperature of environmental exposure was kept at 30 and 50°C constantly. The concentration of H_2SO_4 solution was 10% mass fraction. An interval time, the specimens were taken out for pull-off test.

The adhesion strength between the lining material of the neat and the epoxy-silica nanocomposites and the concrete substrate was measured by the pull-off of the cored samples using the automatic adhesion tester (Elcometer F510S (Elcometer, UK) pull-off adhesion tester) in accordance with ASTM D7234-19 [42]. According to the standard, the linings and concrete substrate were core-cut through lining repair material to at least 10 mm below the interface. A cylindrical steel disk of 50 mm diameter was glued to using epoxy adhesive. Then, the pull-off load from the tensile loading device was applied to the tested specimen with a rate of 0.05 MPa/s until failure occurred. During the test, the load on the fixture was increased in a manner that was as smooth and continuous as possible. The pull-off adhesive strength was calculated by dividing the tensile pull-off load at failure by the circular cutting area of the tested specimen. The failure modes were recorded. If the failure occurred at the concrete–lining interface, then, the true bond strength could be assessed. If the

Table 2: Concrete mix design and properties.

W/C[a]	Constituents[c] (kg.m^{-3})							
	Cement[b]	Aggregates				Total	Superplasticizer	Compressive strength, (MPa)
		Crushed aggregate (max. 10 mm)	Crushed manufactured sand	Natural river sand	Natural fine sand			
0.42	415	748	372	478	287	1885	4.2	62

[a]Water/cement mass ratio. [b]Constituents are given as mass ratio needed to form 1 m^3 of concrete. [c]Vietnamese standard Portland cement (PCB40).

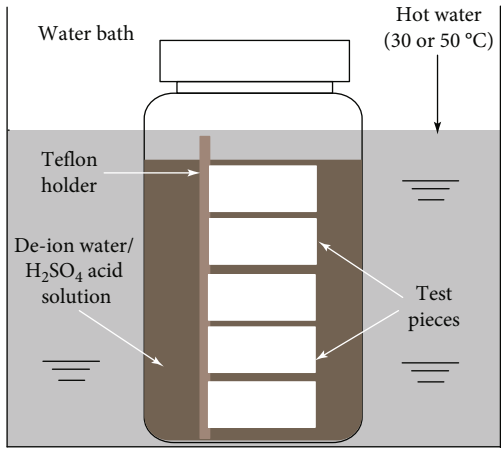

Figure 1: Schematic of the mass uptake apparatus.

failure occurred in either the concrete substrate or lining material, then, the tensile strength of the failing material could be assessed and the interface bond strength was understood to be higher than the value achieved. At least three valid tests were completed, and the results averaged for any particular failure mode. Equation (7) was used to calculate the pull-off bond strength.

$$f_{\text{bond}} = \frac{P_{\text{failure}}}{A}, \tag{7}$$

where P_{failure} is the load at failure and A is the pull-off area.

2.6. Characterization. The phase identification of the incorporated SiO_2 nanoparticles in the epoxy matrix was determined by an X-ray diffractometer (Shimadzu XRD-6100, Japan) with CuKα as radiation source ($\lambda = 1.5405$ angstrom) with a scanning rate of 2° per min and 2theta (2θ) angle range from 10° to 60° at current 30.0 mA and voltage 40.0 kV. Transmission Electron microscope (TEM) photographs were taken with a JEOL JEM 2010F using an acceleration voltage of 200 kV. The penetration depth of the sulfur (S) element was monitored using the coupled Scanning Electron Microscopy (SEM)/Energy dispersive X-ray spectrometer (EDS) JEOL JSM-5310LV analysis of the cross-section of the immersed samples in sulfuric acid.

3. Results and Discussion

3.1. Presence of Incorporated Nanosilica Particle. The XRD patterns for the epoxy-SiO_2 nanocomposites samples (ESP-3) is shown in Figure 3. The broad peak 15-20 degree contributes to the amorphous nature of the epoxy while the diffraction peak at $2\theta = 27.44°$ found in epoxy-silica nanocomposites corresponds to the crystalline nature of SiO_2 particles. It implies that the silica nanofillers embedded in the epoxy matrix.

The peak was shifted to a lower value (18.47°) when nanosilica incorporated in the epoxy base, indicating the epoxy was seemly intercalated into the nanosilica during nanocomposite fabrication. It could lead to expand or exfoliate the nanosilica particles.

TEM images of the sample containing 3 phr of nanosilica are shown in Figures 4(a) and 4(b). The dark lines considered to be the cross-section of silicate and confirm that there is prevalent of single exfoliated silicate layers. The silica was well dispersed throughout the polymer with some agglomeration (see Figure 4(a)) while at close view by high magnification TEM (Figure 4(b)); there were two types of regions: one consisting of both intercalated and exfoliated structures and another consisting both intercalated tactoids and a few individual layers.

From the evidence obtained by XRD and TEM analysis, it can be concluded that although the full exfoliation was not attained, the fabricated silica-epoxy composites are nanocomposites.

3.2. Environmental Uptake Behavior. The materials (neat epoxy, silica-epoxy nanocomposite) immersed into water and into the 10.0 wt.% sulfuric acid solution at 30°C and 50°C. The gained weight at the time (M_t) comparing to the saturated weight (M_∞) due to the solution uptake versus the square root of time over the thickness of samples are plotted as seen in Figures 5–8. It can see that (M_t/M_∞) increased linearly with square root times per thickness before saturation occurred exception of the epoxy-silica nanocomposite immersed in the 10 wt.% H_2SO_4 solution at 50°C. A second stage of diffusion seems to have occurred when the nanocomposite samples immersed in the acid solution at 50°C after about 943 hours. Noticeably, the diffusion coefficient, D, is estimated by using Equation (4). The mass uptake at the equilibrium for the neat epoxy is around 1.78% for immersion in water and around 11.87% for immersion in the H_2SO_4 acid solution when the temperature was 30°C. An increase in temperature increased equilibrium uptake.

The higher order of the mass uptake at the equilibrium for immersion in the sulfuric acid is due to the formation of tertiary amine salts [43]. The equilibrium only attained when all the amines in the resins converted to amine salts [44]. The mass uptake at the equilibrium of the nanosilica samples, for both immersed into water and into the H_2SO_4 solution, was higher order than those of the neat epoxy samples may be

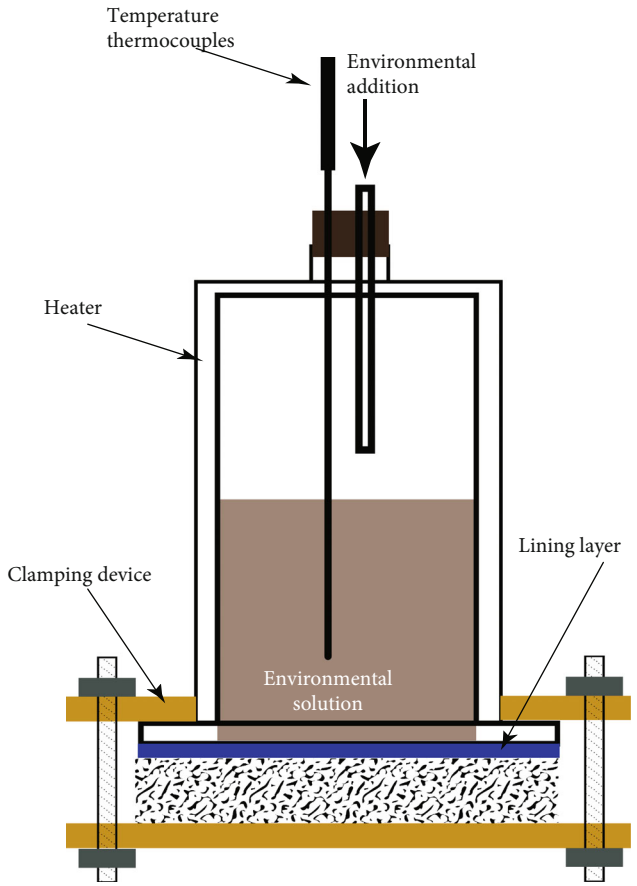

Figure 2: Schematic of the adhesion degradation test apparatus.

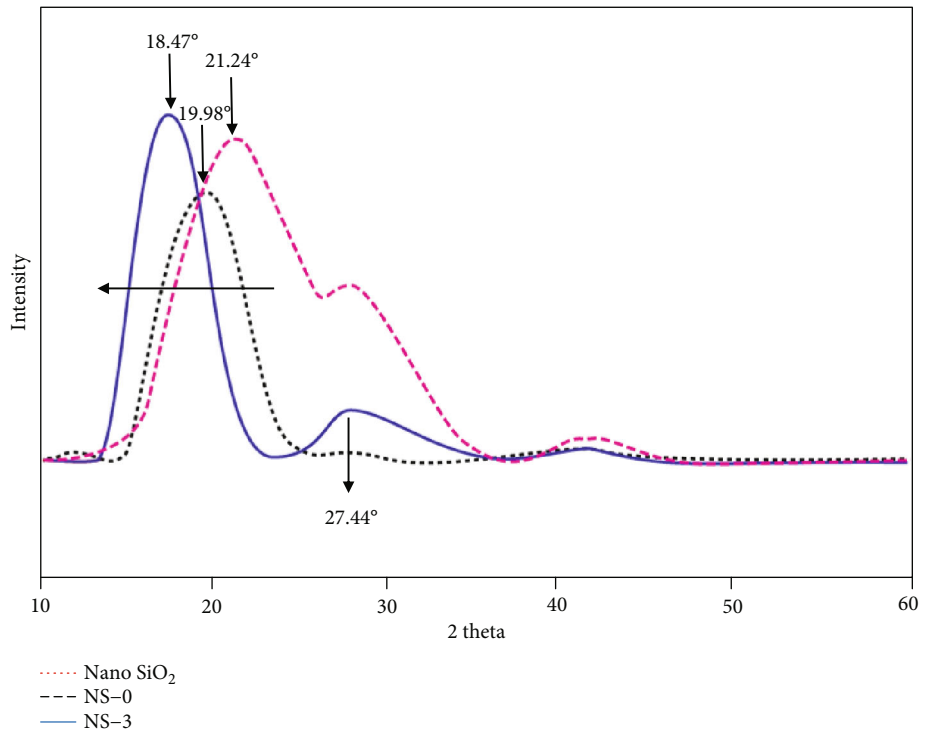

Figure 3: XRD patterns of the samples.

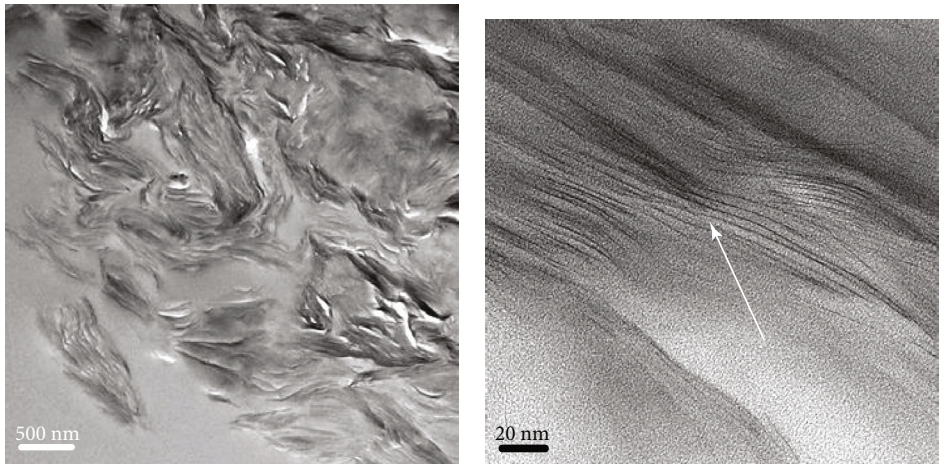

Figure 4: TEM images of (a) NS-0 and (b) NS-3.

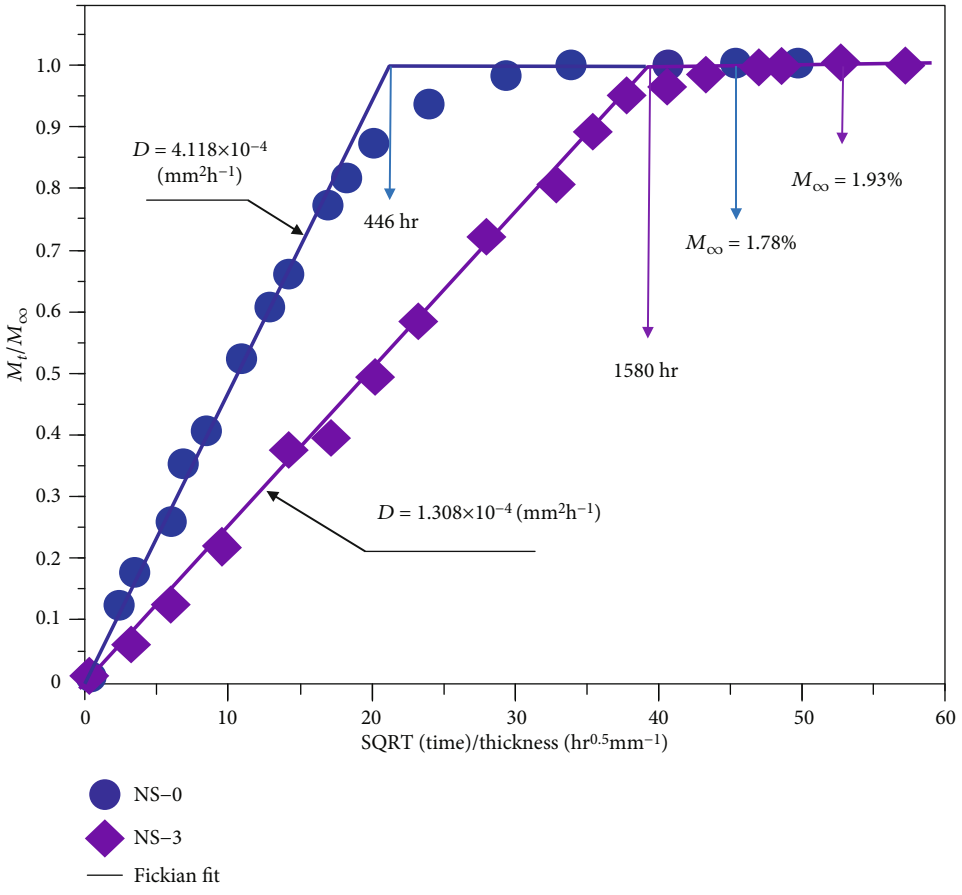

Figure 5: Mass gained in the de-ion water at 30°C as a function of square root time.

due to the higher density of free volume and/or microvoid resulted from agglomerations of the nanosilica particles within the epoxy base as found by the XRD analysis or from the change of viscosity of the mixture and the evaporation of the solvents during the fabrication process. As expected, the performance regarding the enhancement of the barrier to water and the acid solution of the added nanosilica samples is confirmed. The diffusion rate of environmental molecules into the nanocomposites was smaller than those into the neat epoxy. The incorporation of the nanosilica increased the tortuosity path may be contributed to this improvement.

3.3. The H_2SO_4 Penetrated Depth. The sulfuric acid solution consists of H_2SO_4 and water components. EDS combined

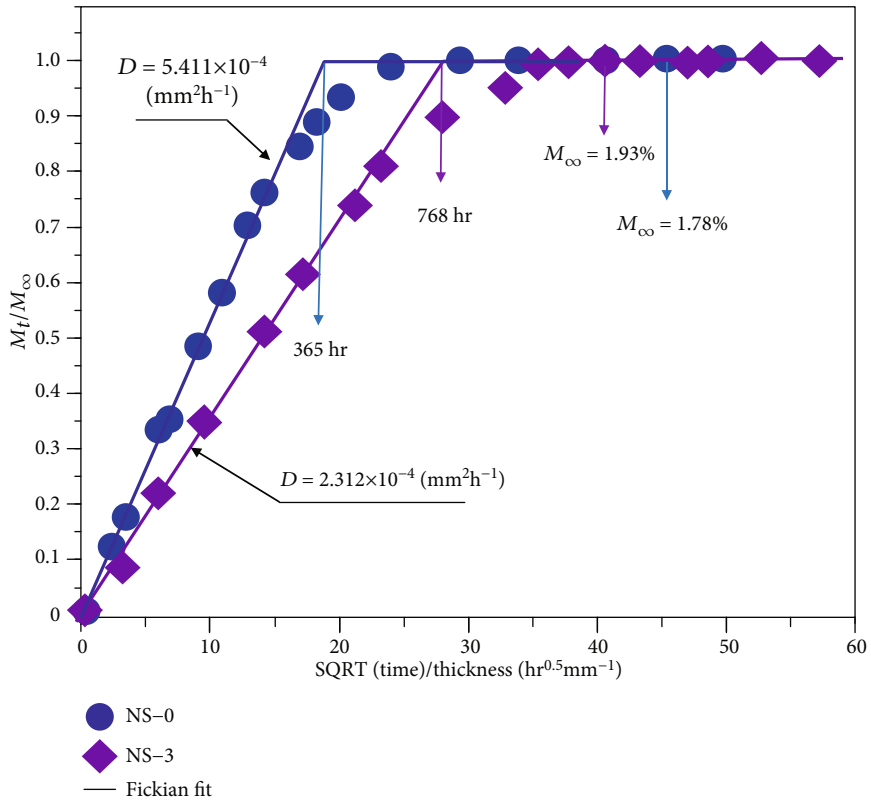

Figure 6: Mass gained in the de-ion water at 50°C as a function of square root time.

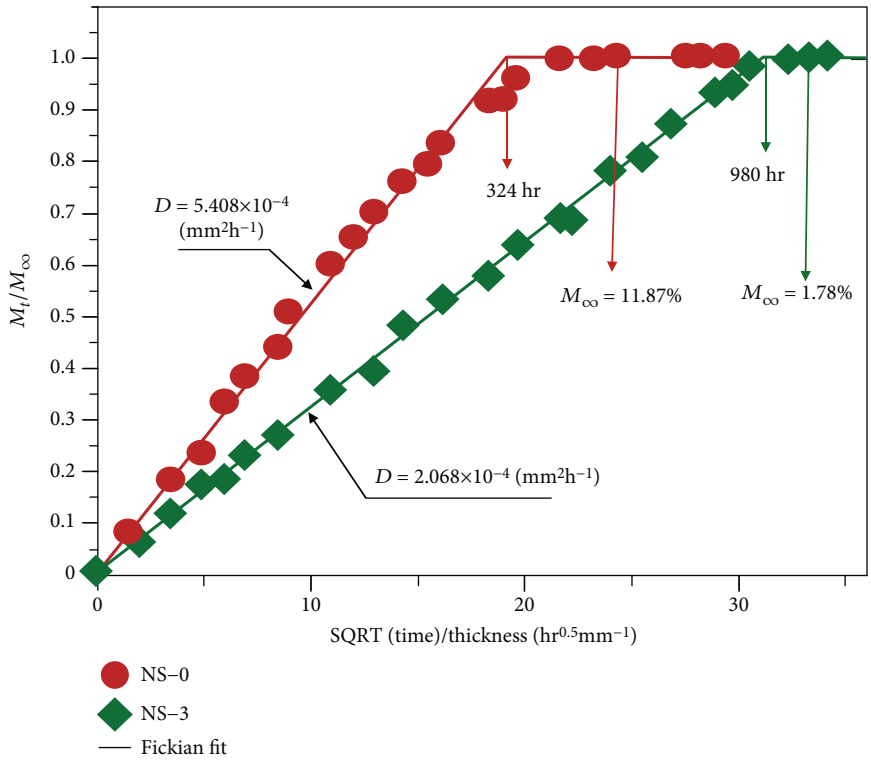

Figure 7: Mass gained in the H_2SO_4 10 wt.% at 30°C as a function of square root time.

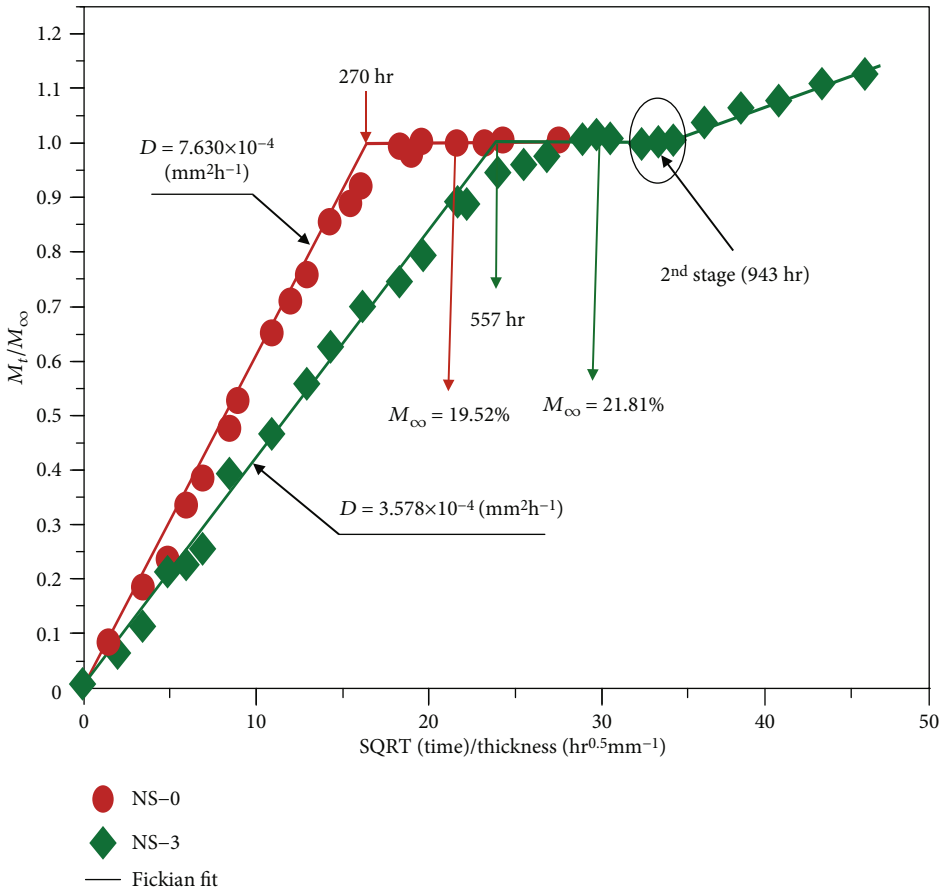

Figure 8: Mass gained in the H_2SO_4 10 wt.% at 50°C as a function of square root time.

SEM analysis used for investigation of the penetration of the H_2SO_4 component to the samples by detection of sulfur element (S) on cutting cross-section of the immersed samples. Figure 9 shows a typical image of the penetrated S distribution within the immersed samples. Figures 10 and 11 present the penetration depth as a function of the square root of time. It can see that the depth is linearly proportional to the square root of immersion time. If the penetration rate, λ, can be defined as the slope of the penetration depth (mm) and the square root time (hour), the penetration rate can be estimated (see Figures 10 and 11). The results are in accordance with the diffusion rate, meaning that H_2SO_4 molecules diffused into the materials along with water molecules.

3.4. Deterioration of Adhesion Strength. The efficiency of adhesion depends on many factors, such as surface treatment, chemical composition and viscosity of the adhesive, application technique, and hardening or cross-linking process of the adhesive itself. Adhesion mechanisms primarily consist of interlocking of the adhesive with the surface of the support with the formation of chemical bonds between polymer and support. For the case of epoxy-, epoxy-silica nanocomposite linings, the governing adhesion mechanisms are mechanical interlocking and chemical bonding.

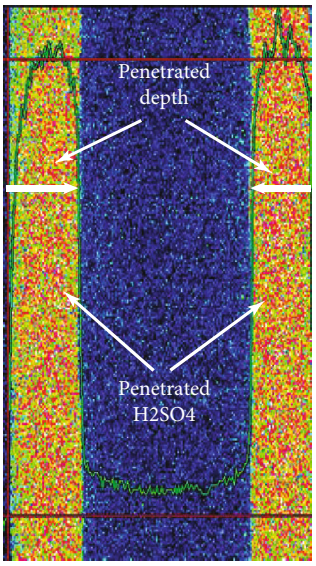

Figure 9: An EDS analysis results of penetrated sulfur element layer in the polymer.

Figure 12 shows the relationship between average bond strength and the square root of time for specimens exposed to the 10 wt.% H_2SO_4 solution at 30°C and 50°C. The results

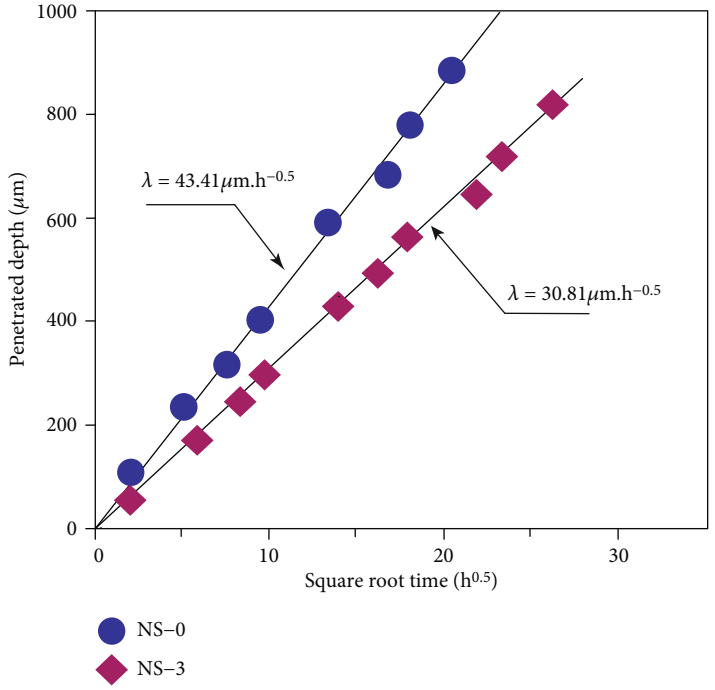

Figure 10: Penetration depth of the H_2SO_4 at 30°C vs. immersion time.

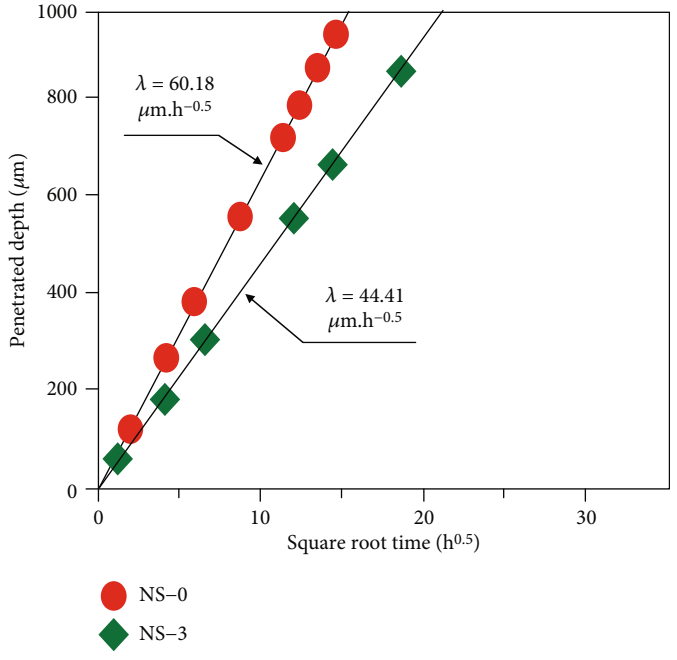

Figure 11: Penetration depth of the H_2SO_4 at 50°C vs. immersion time.

show that the degradation behavior of bond strength consists of the remaining stage and the reduction stage. An enhancement of the bond strength for the epoxy-silica nanocomposite comparing to the neat epoxy was observed. The initial bond strength of the composite lining was about 3.37 MPa, 20% higher than those for the neat epoxy lining.

During exposure to the H_2SO_4 solution, even though experimental scatter of the results, there was no obvious reduction in bond strength up to the time of the equilibrium. This indicates that no harmful effect of the 10 wt.% H_2SO_4 on the cohesion between the lining and the concrete substrate surface due to the barrier function of the linings. Because of the better barrier feature, the bond strength of the nanocomposite lining remained up to 20.6 months and 15.4 months whereas the bond strength of the neat epoxy lining remained only up to 8.2 months and 4.1 months at 40°C and 60°C,

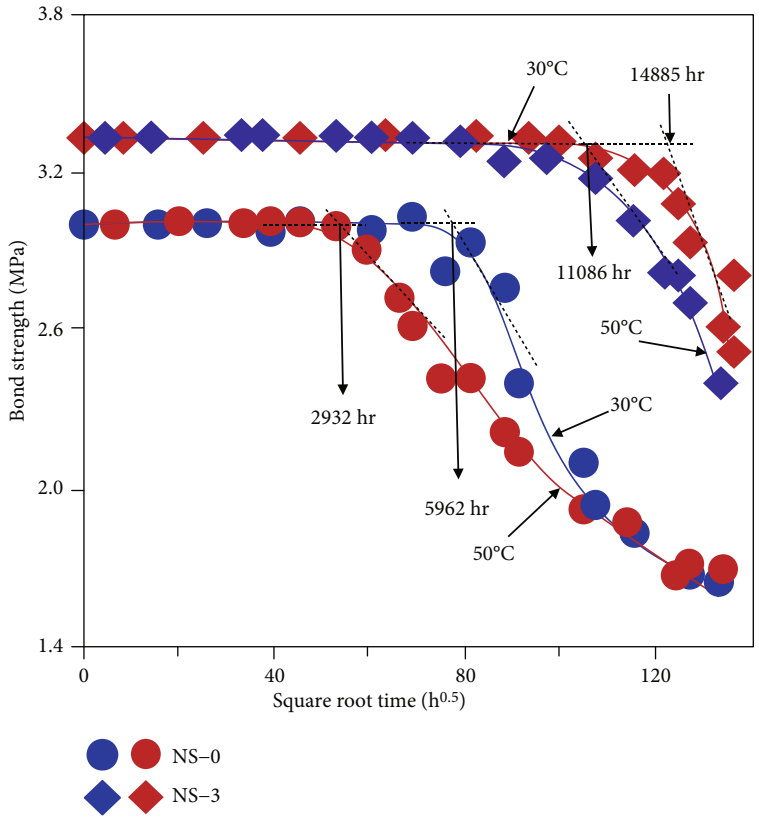

Figure 12: Adhesion behavior of lined epoxy and epoxy-silica nanocomposite lined on concrete substrate exposure of the 10 wt.% H_2SO_4 solution.

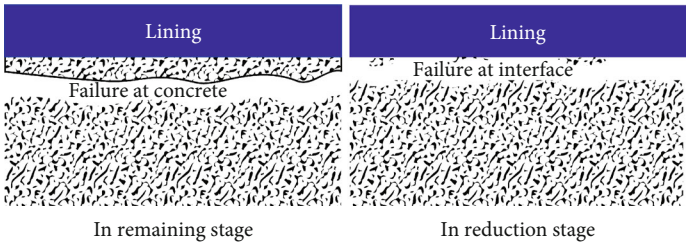

Figure 13: Demonstrate of failure modes.

respectively. Thus, the presence of the incorporated silica nanoparticles in the epoxy matrix was the improvement of the bond strength as well as lengthen the lining service life. The failure mode transited from at the concrete to at the interface in the reduction stage for both lining types (see Figure 13). The sulfur elements on the interfaces of the samples in the reduction stage were observed by EDS analysis (Figure 14). This may confirm the degradation of adhesion strength resulted from the interface corrosion caused by sulfuric acid and water.

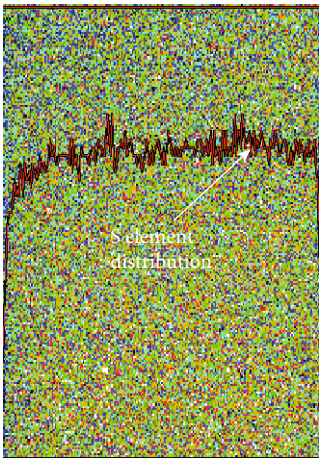

Figure 14: EDS analysis image of the sulfur elements on the pull-off surface of the lining.

4. Conclusions

Based on the results of experiments performed on the protective linings made of epoxy-silica nanocomposites, the following conclusions can be drawn:

(1) The epoxy-silica nanocomposites fabricated was of an inhomogeneous degree of exfoliation with a rather high degree of intercalation. The presence of the nanosilica can significantly improve the barrier properties to water and H_2SO_4 acid solution. The cohesion improvement of nanocomposite lining obtained, about 20% higher in comparison with the neat epoxy lining

(2) The penetration rate of H_2SO_4 acid into the linings was estimated regarding to its diffusion into the linings

(3) Deterioration behavior of the lining's bond strength was investigated. The silica nanocomposites lining showed advancement in the remain of the cohesion on the concrete surface

Data Availability

The data used to support the findings of this study are available from the corresponding author upon request.

Conflicts of Interest

The author declares that there is no conflict of interest regarding the publication of this paper.

Acknowledgments

The author is grateful for the financial support from the Department of Science and Technology of the People's Committee of Hanoi City (Vietnam) under Project No. TC.03-2016-03.

References

[1] X. Li, U. Kappler, G. Jiang, and P. L. Bond, "The ecology of acidophilic microorganisms in the corroding concrete sewer Environment," *Frontiers in Microbiology*, vol. 8, 2017.

[2] W. Kaempfer and M. Berndt, "Polymer modified mortar with high resistance to acid and to corrosion by biogenous sulphuric acid," in *Proceedings of the IXth ICPIC Congress*, pp. 681–687, Bologna, Italy, September 1998.

[3] J. B. Soebbing, R. R. Skabo, H. E. Michel, G. Guthikonda, and A. H. Sharaf, "Rehabilitating water and wastewater treatment plants," *Journal of Protective Coatings & Linings*, vol. 13, pp. 54–64, 1996.

[4] C. D. Parker, "The corrosion of concrete 2. The function of Thiobacillus concretivorus (nov. spec.) in the corrosion of concrete exposed to atmospheres containing hydrogen sulphide," *Australian Journal of Experimental Biology & Medical Science*, vol. 23, 1945.

[5] C. D. Parker, "The corrosion of concrete," *Australian Journal of Experimental Biology & Medical Science*, vol. 23, no. 2, pp. 81–90, 1945.

[6] C. Parker, "Species of sulphur bacteria associated with the corrosion of concrete," *Nature*, vol. 159, no. 4039, pp. 439-440, 1947.

[7] A. K. Parande, P. L. Ramsamy, S. Ethirajan, C. R. K. Rao, and N. Palanisamy, "Deterioration of reinforced concrete in sewer environments," *Proceedings of the Institution of Civil Engineers - Municipal Engineer*, vol. 159, no. 1, pp. 11–20, 2006.

[8] J. Monteny, E. Vincke, A. Beeldens et al., "Chemical, microbiological, and in situ test methods for biogenic sulfuric acid corrosion of concrete," *Cement and Concrete Research*, vol. 30, no. 4, pp. 623–634, 2000.

[9] L. Zhang, P. de Schryver, B. de Gusseme, W. de Muynck, N. Boon, and W. Verstraete, "Chemical and biological technologies for hydrogen sulfide emission control in sewer systems: a review," *Water Research*, vol. 42, no. 1-2, pp. 1–12, 2008.

[10] J. L. Davis, D. Nica, K. Shields, and D. J. Roberts, "Analysis of concrete from corroded sewer pipe," *International Biodeterioration and Biodegradation*, vol. 42, no. 1, pp. 75–84, 1998.

[11] A. P. Harrison Jr., "The Acidophilic thiobacilli and other acidophilic bacteria that share their habitat," *Annual Review of Microbiology*, vol. 38, no. 1, pp. 265–292, 1984.

[12] R. L. Islander, J. S. Devinny, F. Mansfeld, A. Postyn, and H. Shih, "Microbial ecology of crown corrosion in sewers," *Journal of Environmental Engineering*, vol. 117, no. 6, pp. 751–770, 1991.

[13] D. Nica, J. L. Davis, L. Kirby, G. Zuo, and D. J. Roberts, "Isolation and characterization of microorganisms involved in the biodeterioration of concrete in sewers," *International Biodeterioration & Biodegradation*, vol. 46, no. 1, pp. 61–68, 2000.

[14] G. Jiang, J. Sun, K. R. Sharma, and Z. Yuan, "Corrosion and odor management in sewer systems," *Current Opinion in Biotechnology*, vol. 33, pp. 192–197, 2015.

[15] A. A. Almusallam, F. M. Khan, S. U. Dulaijan, and O. S. B. al-Amoudi, "Effectiveness of surface coatings in improving concrete durability," *Cement and Concrete Composites*, vol. 25, no. 4-5, pp. 473–481, 2003.

[16] C. Vipulanandan and J. Liu, "Performance of polyurethane-coated concrete in sewer environment," *Cement and Concrete Research*, vol. 35, no. 9, pp. 1754–1763, 2005.

[17] J. Liu and C. Vipulanandan, "Long-term performance of epoxy coated clay bricks in sulfuric acid," *Journal of Materials in Civil Engineering*, vol. 16, no. 4, pp. 349–355, 2004.

[18] W. Liu, S. V. Hoa, and M. Pugh, "Water uptake of epoxy–clay nanocomposites: Model development," *Composites Science and Technology*, vol. 68, no. 1, pp. 156–163, 2008.

[19] M. Zhi Rong, M. Qiu Zhang, H. Liu, H. Zeng, B. Wetzel, and K. Friedrich, "Microstructure and tribological behavior of polymeric nanocomposites," *Industrial Lubrication and Tribology*, vol. 53, no. 2, pp. 72–77, 2001.

[20] C. B. Ng, L. S. Schadler, and R. W. Siegel, "Synthesis and mechanical properties of TiO_2-epoxy nanocomposites," *Nanostructured Materials*, vol. 12, no. 1-4, pp. 507–510, 1999.

[21] C. B. Ng, B. J. Ash, L. S. Schadler, and R. W. Siegel, "A study of the mechanical and permeability properties of nano- and Micron-Tio2Filled epoxy composites," *Advanced Composites Letters*, vol. 10, no. 3, pp. 101–111, 2001.

[22] X. Shi, T. A. Nguyen, Z. Suo, Y. Liu, and R. Avci, "Effect of nanoparticles on the anticorrosion and mechanical properties of epoxy coating," *Surface and Coatings Technology*, vol. 204, no. 3, pp. 237–245, 2009.

[23] S. Palraj, M. Selvaraj, K. Maruthan, and G. Rajagopal, "Corrosion and wear resistance behavior of nano-silica epoxy composite coatings," *Progress in Organic Coatings*, vol. 81, pp. 132–139, 2015.

[24] M. M. A. Nikje, M. R. Khanmohammadi, A. B. Garmarudi, and M. Haghshenas, "Nanosilica reinforced epoxy floor coating composites: preparation and thermophysical characterization," *Current Chemistry Letters*, vol. 1, pp. 13–20, 2012.

[25] L. Luo, Q. Ma, Q. Wang, L. Ding, Z. Gong, and W. Jiang, "Study of a Nano-SiO_2 microsphere-modified basalt flake epoxy resin coating," *Coatings*, vol. 9, no. 3, p. 154, 2019.

[26] T. C. Wong and L. J. Broutman, "Water in epoxy resins part II. Diffusion mechanism," *Polymer Engineering and Science*, vol. 25, no. 9, pp. 529–534, 1985.

[27] P. Moy and F. E. Karasz, "Epoxy-water interactions," *Polymer Engineering and Science*, vol. 20, no. 4, pp. 315–319, 1980.

[28] N. L. Thomas and A. H. Windle, "A deformation model for case II diffusion," *Polymer*, vol. 21, no. 6, pp. 613–619, 1980.

[29] H. L. Frisch, "Sorption and transport in glassy polymers–a review," *Polymer Engineering and Science*, vol. 20, no. 1, pp. 2–13, 1980.

[30] A. Peterlin, "Diffusion with discontinuous swelling. IV. Type II diffusion into spherical particles," *Polymer Engineering and Science*, vol. 20, no. 4, pp. 238–243, 1980.

[31] C. M. Hansen, "Diffusion in polymers," *Polymer Engineering and Science*, vol. 20, no. 4, pp. 252–258, 1980.

[32] G. Astaluta and G. C. Sarti, "A class of mathematical models for sorption of swelling solvents in glassy polymers," *Polymer Engineering and Science*, vol. 18, no. 5, pp. 388–395, 1978.

[33] J. M. Vergnaud, "Liquid transport processes in polymeric materials," in *Modeling and Industrial Applications*, p. 362, Prentice-Hall, Upper Saddle River, NJ, USA, 1991.

[34] J. Crank, *The Mathematics of Diffusion*, Clarendon Press, Oxford, UK, 1975.

[35] C. H. Shen and G. S. Springer, "Moisture absorption and desorption of composite material," *Journal of Composite Materials*, vol. 10, no. 1, pp. 1–10, 1976.

[36] H. Lee and K. Neville, *Epoxy resins, their Applications and Technology*, McGaw-Hill, New York, NY, USA, 1957.

[37] M. G. Lu, M. J. Shim, and S. W. Kim, "Effects of moisture on properties of epoxy molding compounds," *Journal of Applied Polymer Science*, vol. 81, no. 9, pp. 2253–2259, 2001.

[38] L. Núñez, M. Villanueva, F. Fraga, and M. R. Núñez, "Influence of water absorption on the mechanical properties of a DGEBA (n = 0)/1, 2 DCH epoxy system," *Journal of Applied Polymer Science*, vol. 74, no. 2, pp. 353–358, 1999.

[39] TCVN9113, *Reinforced concrete pipes for water draining*, Ministry of Construction, Vietnam, 2012.

[40] A. P. Joseph, J. Keller, H. Bustamante, and P. L. Bond, "Surface neutralization and H_2S oxidation at early stages of sewer corrosion: influence of temperature, relative humidity and H_2S concentration," *Water Research*, vol. 46, no. 13, pp. 4235–4245, 2012.

[41] Institute, ICR, *Selecting and specifying concrete surface preparation for sealers, coatings, polymer overlays, and concrete repair*, ICRI Committee 310, Rosemont, IL, USA, 2013.

[42] A. Standards, "Standard Test Method for Pull-Off Adhesion Strength of Coatings on Concrete Using Portable Pull-Off Adhesion Testers," in *American Society for Testing and Materials Annual Book of ASTM Standards*, West Conshohocken, PA, USA, ASTM International, 2019.

[43] S. Ono, K. Tsuda, M. Kubouchi, T. Nishiyama, and H. Hojo, "Degradation behavior of amine cured epoxy resin and FRP in acid solutions," in *Proceeding of the Tenth International Conference on composite materials*, pp. 215–222, Whistler, Canada, 1995.

[44] K. Tsuda and M. Kubouchi, "Decomposition of polymeric materials," *Corrosion Engineering*, vol. 44, pp. 141–154, 1995.